ACCELERATED PUBLICATION

Monitoring conformational changes of proteins in cells by fluorescence lifetime imaging microscopy

Véronique CALLEJA*†, Simon M. AMEER-BEG†, Borivoj VOJNOVIC†, Rudiger WOSCHOLSKI‡, Julian DOWNWARD§ and Banafshé LARIJANI*[1]

*Cell Biophysics Laboratory, London Research Institute, Cancer Research UK, Lincoln's Inn Fields Laboratory, 44 Lincoln's Inn Fields, London WC2A 3PX, U.K., †Advanced Technology Development Group, Gray Cancer Institute, Mount Vernon Hospital, Northwood, Middx. HA6 2JR, U.K., ‡Department of Biological Sciences, Biochemistry Building, South Kensington Campus, Imperial College London, London SW7 2AZ, U.K., and §Signal Transduction Laboratory, London Research Institute, Cancer Research UK, Lincoln's Inn Fields Laboratory, 44 Lincoln's Inn Fields, London WC2A 3PX, U.K.

To be able to detect *in situ* changes in protein conformation without perturbing the physiological environment would be a major step forward in understanding the precise mechanism occurring in protein interaction. We have developed a novel approach to monitoring conformational changes of proteins in intact cells. A double-labelled fluorescent green fluorescent protein–yellow fluorescent protein (GFP–YFP) fusion protein has been constructed, allowing the exploitation of enhanced-acceptor-fluorescence (EAF)-induced fluorescence resonance energy transfer (FRET). Additionally, a novel fusion partner, YFP^{dark}, has been designed to act as a sterically hindered control for EAF-FRET. Any conformational changes will cause a variation in FRET, which, in turn, is detected by fluorescence lifetime imaging microscopy ('FLIM'). Protein kinase B (PKB)/Akt, a key component of phosphoinositide 3-kinase-mediated signalling, was selected for this purpose. Although conformational changes in PKB/Akt consequent to lipid binding and phosphorylation have been proposed in models, its behaviour in intact cells has not been tractable. We report here that platelet-derived-growth-factor ('PDGF') stimulation of NIH3T3 cells expressing the GFP–Akt–YFP construct resulted in a loss of FRET at the plasma membrane and hence a change in PKB/Akt conformation. We also show that the GFP–Akt–YFP construct conserves fully its functional integrity. This novel approach of monitoring the *in situ* conformational changes has broad application for other members of the AGC kinase superfamily and other proteins.

Key words: AGC kinases, enhanced acceptor fluorescence, conformational change, dark yellow fluorescent protein (YFP^{dark}), fluorescence resonance energy transfer (FRET), protein kinase B (PKB)/Akt.

INTRODUCTION

The ability to detect *in situ* changes in protein conformation without perturbing the cellular environment would give new insight into the precise mechanisms occurring in protein interactions. For this purpose, we have selected protein kinase B (PKB)/Akt, a member of the AGC kinase superfamily, which plays an important role in phosphoinositide 3-kinase-mediated cellular signalling such as cell survival and growth [1].

In order to investigate intramolecular conformational changes of PKB/Akt, we introduced two different fluorophores, green fluorescent protein (GFP) and yellow fluorescent protein (YFP) respectively, on either end of PKB/Akt to create a double fluorescent-tagged construct, GFP–Akt–YFP. Fluorescence resonance energy transfer (FRET) between spectrally similar GFP molecules in single cells has been demonstrated previously [2]. FRET induced by enhanced acceptor fluorescence (EAF) results in the increase of the combined fluorescence lifetime of both donor and acceptor. To control for EAF induced FRET we have used a new dark YFP (YFP^{dark}) fused to make the GFP–Akt–YFP^{dark} construct, which allows verification of these types of measurements using the full-length protein. This variation in FRET is measured by fluorescence lifetime imaging microscopy (FLIM) and is thus independent of local concentration variations [3,4].

The activation of PKB/Akt and its subsequent translocation to the membrane is dependent on the integrity of its N-terminal pleckstrin homology (PH) domain, which binds to the phosphoinositide 3-kinase-generated second messengers PtdIns(3,4,5)P_3 and PtdIns(3,4)P_2 [5]. In addition, PKB/Akt is subject to regulation by phosphorylation, a feature shared with most members of the AGC superfamily growth [1,6]. Two important regulatory sites for full Akt activation have been identified so far: Thr^{308} in the kinase domain and Ser^{473} in the hydrophobic motif of the C-terminal part [7]. Recent crystal-structure studies [8,9] indicated that conformational changes within PKB/Akt regulate its lipid binding and activity [1].

In the present study we show that the change in the intramolecular proximity of GFP and YFP causes a variation in FRET coupling efficiency, which is, in turn, imaged in cells using FLIM. Thus, for the first time, using this particular methodology, conformational change of a full-length protein kinase in response to a growth factor can be monitored *in situ*.

EXPERIMENTAL

DNA constructs and expression vectors

The pEGFP–C1–GFP–Akt fusion construct, where GFP is fused in N-terminus of haemagglutinin A-tagged mouse Akt1, was

Abbreviations used: PKB, protein kinase B; GSK3, glycogen synthase kinase; EGFP, enhanced green fluorescent protein; YFP, yellow fluorescent protein; YFP^{dark}, dark YFP; EYFP, enhanced YFP; PH, pleckstrin homology; PDGF, platelet-derived growth factor; EAF, enhanced acceptor fluorescence; FRET, fluorescence resonance energy transfer; FLIM, fluorescence lifetime imaging microscopy.

[1] To whom correspondence should be addressed (e-mail b.larijani@cancer.org.uk).

made as previously described [10]. The YFP–Akt construct was made by cutting out YFP from pEYFP-N1 (Clontech) using restriction endonucleases *Nhe*I/*Bsr*GI and was placed instead of the enhanced GFP (EGFP) in the pEGFP–C1–GFP–Akt construct in the *Nhe*I/*Bsr*GI sites. GFP–Akt from pEGFP–C1–GFP–Akt was PCR-amplified using the sense oligonucleotide 5′-AGAGGATCCGCCGCCACCATGGTGAGCAAGGGCGAGG-AGCTGTTCACCGGG-3′ and the antisense oligonucleotide 5′-ATCGAATTCTCCGCCACCTCCACCTCCGGTGTGCCAC-TGGCTGAGTAGGAGAACTGGGG-3′, cut with *Bam*HI/ *Eco*RI and introduced as an N-terminal fusion in a pCDNA3 vector containing enhanced YFP (EYFP; kindly provided by Dr Thomas Gudermann, Institut für Pharmakologie und Toxikologie, Philipps Universität Marburg, Marburg, Germany [11]) in *Bam*HI/*Eco*RI sites to make the GFP–Akt–YFP construct. A linker formed of six glycine residues separates N-terminal EGFP from Akt and C-terminal EYFP from Akt in GFP–Akt–YFP. An environmentally stable (red-shifted) form of EYFP [12] was made by replacing the glutamine residue at position 70 of EYFP by a methionine residue. Site-directed mutagenesis was performed by using the QuikChange mutagenesis kit (Stratagene). All the constructs described above were made with the $Gln^{70} \rightarrow$ Met mutation on EYFP. $EYFP^{dark}$ was made by replacing Tyr^{67} in the EYFP chromophore with a leucine residue. This mutation quenches the fluorescence emission of EYFP.

Immunoprecipitation and *in vitro* GFP–Akt–YFP kinase assay

NIH3T3 cells seeded at 140 000 cells/six-well plate were transfected with the GFP–Akt–YFP construct using LIPOFECTAMINE/PLUS™ reagent (Gibco BRL) and starved in Dulbecco's modified Eagle's medium/0.2 % BSA. After treatment, the cells were lysed for 15 min on ice in lysis buffer [20 mM Tris/HCl (pH 7.4)/150 mM NaCl/100 mM NaF/10 mM $Na_4P_2O_7$/10 mM EDTA, supplemented with 1 mM Na_3VO_4, 1 mM PMSF, 10 μg/ml leupeptin and 10 μg/ml aprotinin]. GFP–Akt–YFP was immunoprecipitated with high-affinity rat monoclonal anti-(haemagglutinin A) antibody (Boehringer-Mannheim) for 2 h at 4 °C on Protein G–Sepharose beads. Immunoprecipitates of GFP–Akt–YFP were washed twice with the lysis buffer and twice with the kinase buffer (1×) [25 mM Tris/HCl (pH 7.5)/5 mM β-glycerophosphate/2 mM dithiothreitol/0.1 mM Na_3VO_4/10 mM $MgCl_2$] [Cell Signaling, New England Biolabs (UK) Ltd.]. GFP–Akt–YFP on beads was incubated for 30 min at 30 °C in 40 μl of kinase buffer 1× and supplemented with 200 μM ATP and 1 μg of glycogen synthase kinase (GSK3) fusion protein (Cell Signaling). GSK3α,β crosstide corresponding to residues surrounding the $Ser^{21/9}$ site (CGPKGPGRRGRRRTSSFAEG) was fused to the N-terminus of paramyocin (Cell Signaling). To terminate the reaction, 13 μl of 4×SDS sample buffer [125 mM Tris/HCl (pH 6.8)/6 % (w/v) SDS/20 % (v/v) glycerol/0.02 % Bromophenol Blue supplemented with 10 % β-mercaptoethanol) was added, and the samples vortex-mixed. The proteins were separated on a SDS/12 %-(w/v)-PAGE gel.

Western-blot analysis

The gels were transferred to PVDF membrane (Immobilon P; Millipore) and incubated in blocking buffer TBS-T [10 mM Tris/HCl (pH 7.4)/150 mM NaCl/0.05 % Tween-20], supplemented with 3 % BSA for 1 h. The membrane was washed in TBS/Triton/1 % milk for 1 h and incubated with the different antibodies; phospho-Akt (Thr^{308}) or phospho-GSK3α,β ($Ser^{21/9}$) antibodies (rabbit polyclonal antibody from Cell Signaling) or phospho-Akt (Ser^{473}) (rabbit polyclonal antibody raised against the C-terminal phosphopeptide HFPQF*p*SYSASS of Akt1) at 1:1000 dilution for 2–3 h in TBS/Triton/3 % BSA. Anti-GFP (mouse monoclonal antibody; CRUK Immunology Group, Paterson Institute for Cancer Research, Christie Hospital, Manchester, U.K.) was used at 1:10 000 dilution for 30 min. The secondary horseradish-peroxidase-conjugated antibodies were used at 1:5000 dilution and proteins revealed by enhanced chemiluminescence (ECL®; Amersham Biosciences).

Confocal microscopy

NIH3T3 cells were seeded at 30 000 cells/well on glass coverslips in 24-well plates and transfected as described above. After treatment the cells were washed twice in PBS and fixed in 4 % paraformaldehyde for 15 min. The coverslips were washed and mounted on the slides with Immuno Floure (ICN Biomedicals, Costa Mesa, CA, U.S.A.). The slides were then analysed by confocal microscopy using a Zeiss laser scanning confocal microscope (LSM 510), an Argon 458/488 laser and a 63× Apochromat oil-immersion objective lens.

Measurement of FRET by FLIM in the frequency domain

A detailed description of the FRET monitored by FLIM can be found elsewhere [3]. We have monitored lifetime detection in the frequency (phase) domain. Phase methods provide an average lifetime where sinusoidally modulated light is used to excite the sample. The lag in the emitted fluorescence signal permits measurement of phase (τ_p) and modulation depth (τ_m) of the fluorescence. The lifetime, $\langle\tau\rangle$, is the average of phase shift and relative modulation depth $(\tau_m + \tau_p)/2$ of the emitted fluorescence signal.

In this particular study, since GFP and YFP are spectrally similar EAF occurs, which, in turn, induces FRET, we monitor the variation in the combined change in lifetime of donor (GFP) and acceptor (red-shifted YFP). The detailed explanation of EAF and its effect on FRET efficiency can be found elsewhere [2,13]. It is noteworthy that, in the present study, FRET is detected when there is an increase in the combined donor and acceptor lifetime, and the absence of FRET is detected by the decrease in lifetime to the uncomplexed donor lifetime. GraphPad InStat software (version 3.0 for Mac-2001) was used for the statistical analysis. An unpaired t test with Welch correction was used to determine the significance of variation in lifetime between GFP–Akt, GFP–Akt–YFP and Akt–YFP (seven or more cells were analysed per experiment; $n = 4$). The P values were determined at 95 % confidence interval.

All images were taken using a Zeiss Plan-Apochromat 100×/1.4-numerical-aperture phase-3 oil-immersion objective, with images recorded at a modulation frequency of 80.218 MHz. The GFP–Akt–YFP was excited using the 488 nm line of an argon/krypton laser and the resultant fluorescence separated using a combination of dichroic beam splitter (Q 505 LP; Chroma Technology Corp., Brattleboro, VT, U.S.A.) and interference filter (HQ510/20; Chroma Technology Corp.)

Time domain

Time-correlated single-photon-counting FLIM was performed using a modified multi-photon microscope system [Bio-Rad MRC 1024MP and Becker & Hickl GmbH (Berlin, Germany) SPC700] described previously [14] in the reverse stop–start

mode. Biological samples were analysed on prepared microscope coverslides and imaged with a 4×1.3-numerical-aperture (Nikon CFI Fluor) oil-immersion objective. Data were collected at 500 ± 20 nm [Coherent Inc. (Santa Clara, CA, U.S.A.) 35–5040 instrument]. Laser power was adjusted to give average photon counting rates of the order 10^4–10^5 photons $\cdot s^{-1}$ (0.0001–0.001 photons/excitation event) and with peak rates approaching 10^6 photons $\cdot s^{-1}$, below the maximum counting rate afforded by the TCSPC (time-correlated single-photon counting) card to avoid pulse pile-up. Samples were imaged for ≈ 120 s to achieve appropriate photon statistics for determination of the fluorescence dynamics. Data was analysed using in-house-developed software tools.

RESULTS

To study intramolecular conformational changes of a full-length protein in intact cells we constructed a double-tagged Akt construct with spectrally similar fluorophores: GFP at the N-terminus and YFP at the C-terminus. Primarily, we wanted to verify whether the GFP–Akt–YFP construct resulted in EAF-induced FRET and also to confirm that variations of lifetime were not due to the multiple decay components of the GFP–Akt–YFP. The appropriate control for the latter was the construction of a YFP the fluorescence emission of which is quenched (YFP^{dark}). YFP^{dark} has Tyr^{67} mutated to leucine. The advantage of using the 'dark' YFP as a control is that it maintains the overall structure of the chimaeric sensor protein.

We show that, in the presence of the YFP^{dark} (GFP–Akt–YFP^{dark}), the lifetime decreases to that of GFP alone, confirming that YFP acts as a proper acceptor in the GFP–Akt–YFP construct. Furthermore, this demonstrates that the quenching of the GFP was not due to its local environment. This decrease is detected in the average lifetime (Figure 1A) and in the two-dimensional histogram, where the blue dot (GFP-Akt-YFP^{dark}) and green dot (GFP-Akt) superimpose and is clearly distinct from that of GFP–Akt–YFP (red; Figure 1B). Figure 1(C) shows that the constructs are expressed as intact species of the correct molecular masses and that, by mutating the YFP, we have not truncated the fused protein. The emission spectra of the different fluorescent constructs in cell lysates obtained with a 710-PTI spectrofluorimeter are shown in Figure 1(D). Samples were excited at 480 nm and the emission spectra scanned from 500 to 640 nm. The maximum emission intensity of the red-shifted YFP–Akt (yellow) is detected at 532 nm, GFP–Akt (pink) is at 512 nm, GFP–Akt–YFP^{dark} (purple) is at 512 nm, and GFP–Akt–YFP (blue) is at 520 nm. The quenched fluorescence emission of the YFP^{dark} is apparent in these spectra, as the GFP–Akt–YFP^{dark} has the same maximum emission as GFP–Akt. A further verification of FRET in GFP–Akt–YFP was performed by using time-domain FLIM. The lifetimes determined via time domain were $\tau_{GFP-Akt} = 2.15 \pm 0.05$ ns, $\tau_{GFP-Akt-YFP} = 2.20 \pm 0.05$ ns and $\tau_{YFP-Akt} = 2.45 \pm 0.05$ ns. Figure 1(E) shows a logarithmic plot of the fluorescence decay of the GFP–Akt–YFP construct. It is clear from the residuals that the decay is bi-exponential (green line on graph). Furthermore, with an unrestrained bi-exponential fit ($\chi^2 = 1.18$), the long-lifetime component of YFP (2.40 ns) and a short component attributable to FRET-quenched GFP (1.13 ns) are recovered. The time domain results suggest that the GFP–Akt–YFP construct undergoes FRET and the changes in lifetime are due to transfer of energy.

Confirmation that FRET occurs between GFP and red-shifted YFP allowed us to examine whether Akt undergoes conformation changes upon stimulation with platelet-derived growth factor (PDGF). We monitored variation in lifetime of GFP–Akt–YFP in intact cells by FLIM. NIH3T3 cells were transiently transfected with GFP–Akt, GFP–Akt–YFP and YFP–Akt fluorescent constructs. The intensity images are shown in the upper panel of Figure 2(A). It must be noted that loss of resolution in the intensity images is due the intrinsic properties of the detector (an image intensifier) used for frequency domain FLIM and the image treatment required for the measurement of lifetime. The images were thresholded in such a manner that the signal-to-noise ratio was systematically 2:1 and therefore the plasma membrane was not eliminated. The lifetime distribution in each case was determined (Figure 2A, lower panel). The average lifetimes are 2.14 ± 0.03 ns, 2.33 ± 0.02 ns and 2.41 ± 0.01 ns for GFP–Akt, GFP–Akt–YFP and YFP–Akt respectively (Figure 2C). The cells transfected with GFP–Akt–YFP undergo FRET induced by EAF. That is, the two fluorophores are in close proximity (< 7 nm) for resonance energy transfer to occur. The two-dimensional histogram illustrates a concomitant increase (upward diagonal shift) in the combined lifetime of GFP–Akt–YFP compared with GFP-Akt (Figure 2B). However, when the GFP–Akt–YFP-transfected cells were treated for 5 min with 30 ng/ml PDGF, a decrease in the lifetime at the plasma membrane from 2.3 ns to 1.7 ns is detected (Figure 2A). The selected lifetime regions of interest further demonstrate this change. The pixels with low lifetime distribution (white, 1.7–2.0 ns) are at the plasma membrane and the pixels with higher lifetime distribution (blue, 2.0–2.5 ns) are in the cytoplasm (Figure 2A, right-hand bottom panels). The loss of energy transfer reflects a separation between the fluorophores and hence a change in Akt conformation. The conformation that results in FRET is referred to as the 'closed' conformation and that with the loss of FRET the 'open' conformation of Akt (Figure 2D).

To confirm the functional integrity of the GFP–Akt–YFP construct, we verified by confocal microscopy that single-tagged GFP–Akt and YFP–Akt as well as GFP–Akt–YFP translocated to the plasma membrane upon PDGF stimulation. This is apparent in the lower panel of Figure 3(A). Moreover, we have demonstrated that Thr^{308} and Ser^{473} are both phosphorylated and the downstream target (GSK3) is also phosphorylated (Figures 3B and 3C). Notably there was no steric hindrance of YFP on Ser^{473} site phosphorylation, since PDGF induced phosphorylation, as did inhibition of protein phosphatase 1/protein phosphatase 2A with okadaic acid (Figure 3C).

To further demonstrate the physiological relevance of the Akt conformational change detected by the decrease of GFP–Akt–YFP lifetime at the plasma membrane, we treated cells with LY294002 (an inhibitor of phosphoinositide 3-kinase). Figure 4(A) shows that, upon PDGF stimulation, there is a loss of FRET ('open' conformation) at the plasma membrane, indicated by the decrease in the GFP–Akt–YFP lifetime from 2.3 to 1.7 ns. In the presence of LY294002, this phenomenon is partially prevented (lifetime at the plasma membrane remains unchanged). Concomitantly, upon LY294002 pretreatment, we observed a decrease in the PDGF-induced GFP–Akt–YFP phosphorylation on Thr^{308} (Figure 4B, upper panel). In the same manner, a decrease in phosphorylation occurs with the endogenous protein (Figure 4B, lower panel).

DISCUSSION

Our interest has been focused on developing a novel way for monitoring *in situ* the change in conformation of a full-length protein. For this purpose we utilized a protein of interest, namely

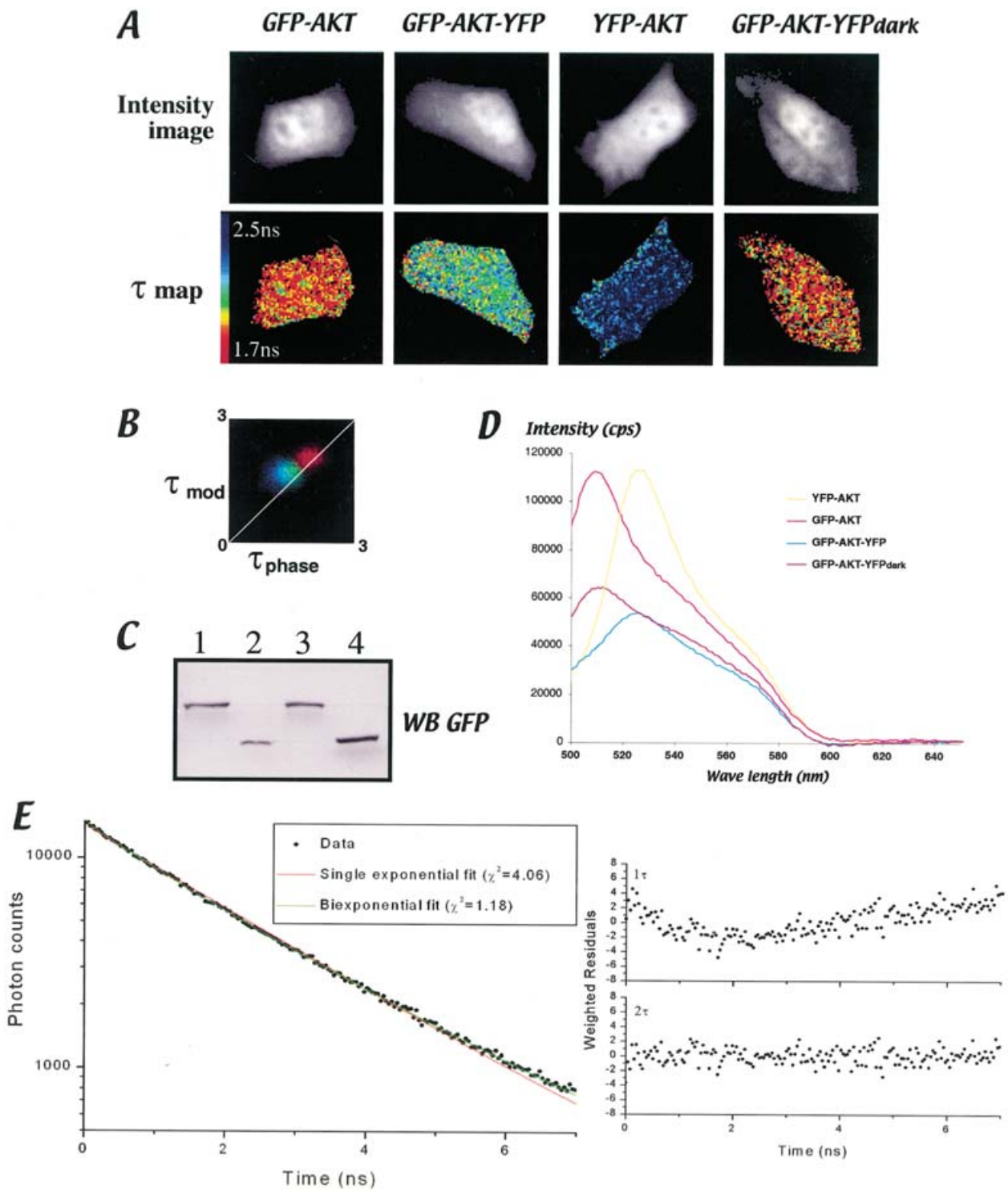

Figure 1 Assessment of FRET in GFP–Akt–YFP by time-domain FLIM and YFP^{dark}

(**A**) Intensity images (top panels) and lifetime maps (bottom panels) of GFP–Akt, GFP–Akt–YFP, YFP–Akt and GFP–Akt–YFP^{dark} in transfected NIH3T3 cells. (**B**) Two-dimensional histograms of (τ_p) and (τ_m) lifetimes obtained in the frequency domain illustrating the variation in lifetime. GFP–Akt (green dot), GFP–Akt-YFP^{dark} (blue dot) and GFP–Akt–YFP (red dot). Note the superimposition of the blue and green dots indicates that GFP–Akt–YFP^{dark} lifetime decreases to the value of GFP–Akt. Hence EAF-induced FRET is due to unquenched YFP in the GFP–Akt–YFP construct. (**C**) Expression of (1) GFP–Akt–YFP, (2) GFP–Akt, (3) GFP–Akt–YFP^{dark} and (4) YFP–Akt constructs was verified by Western blots (WB) with an anti-GFP antibody of a total lysate of NIH3T3 transfected cells. (**D**) Emission spectra of the different fluorescent constructs in cell lysates obtained by a 710-PTI spectrofluorimeter. Samples were excited at 480 nm and the emission spectra scanned from 500 nm to 640 nm. YFP–Akt (yellow), GFP-Akt (pink), GFP-Akt-YFP^{dark} (purple) and GFP–Akt–YFP (blue). The quenched fluorescence emission of the YFP^{dark} is apparent in these spectra. The units of the *y*-axis are counts per photon-second (cps). (**E**) Time-domain FLIM. The fluorescence decay illustrates a logarithmic plot of the fluorescence decay of the GFP–Akt–YFP construct. The data are not adequately fit to a single-exponential-decay model (red line) as evidenced by the χ^2. The 1τ residuals (right-hand plot) indicate at least one additional decay component. Fitting to an unrestrained bi-exponetial decay is clearly more appropriate ($\chi^2 = 1.18$ and residuals). Furthermore, the long-lifetime component of YFP (2.40 ± 0.05 ns) and a short component attributable to FRET-quenched GFP (1.13 ± 0.15 ns) are recovered. This supports the frequency domain data and confirms a mechanism consistent with EAF-FRET.

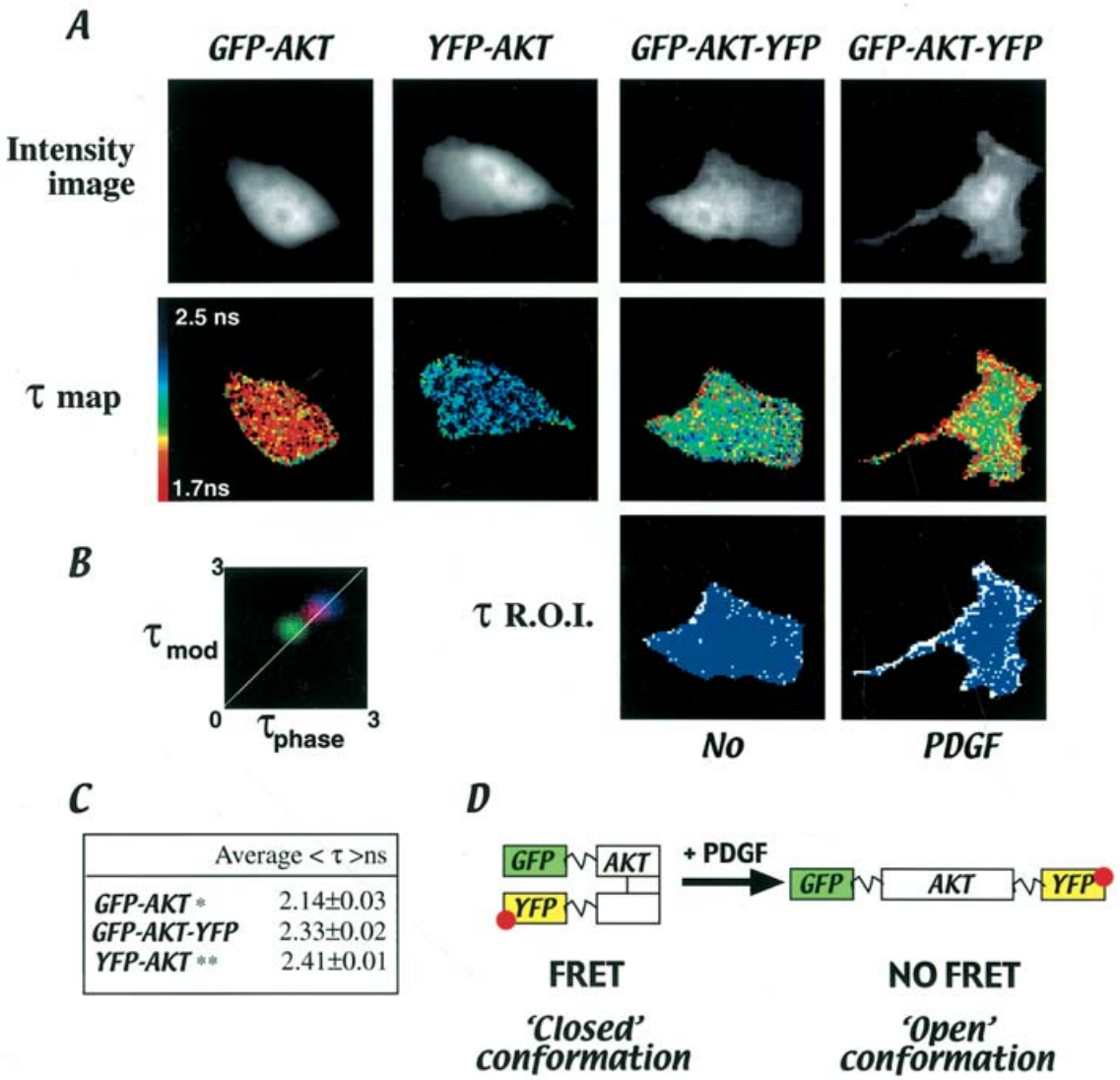

Figure 2 Change in GFP–Akt–YFP conformation upon cell stimulation

(**A**) Intensity images of NIH3T3 cells (top panels) and their corresponding average lifetime $\langle\tau\rangle$ maps (middle panels; see the Experimental section). NIH3T3 cells were transiently transfected with GFP–Akt, YFP–Akt and GFP–Akt–YFP fluorescent constructs. GFP–Akt–YFP-transfected cells were treated for 5 min with 30 ng/ml PDGF where indicated. The lifetime distribution is from 1.7 ± 0.15 ns to 2.5 ± 0.15 ns. Upon stimulation there is a loss of FRET ('open' conformation) at the plasma membrane indicated by the decrease in the GFP–Akt–YFP lifetime. The bottom panels represent two regions of interest (R.O.I.) of lifetimes ranging from 1.7 ns to 2.0 ns (white pixels) and from 2.0 ns to 2.5 ns (blue pixels). (**B**) Two-dimensional histograms of τ_{phase} and τ_{mod} lifetimes obtained in the frequency domain illustrating the variation in lifetime. GFP–Akt (green dot), lowest lifetime; GFP–Akt–YFP (red dot) intermediate lifetime; and YFP–Akt (blue dot), highest lifetime ($n =$ five cells). (**C**) Statistical analysis of the average lifetimes $\langle\tau\rangle$ (see the Experimental section) of GFP–Akt, GFP–Akt–YFP and YFP–Akt. An asterisk (*) indicates an extremely significant increase in the average lifetime of GFP–Akt–YFP compared with GFP–Akt with a P value < 0.0003, $n =$ eight cells at 95 % confidence interval. Two asterisks (**) indicates a very significant difference between the average lifetime of GFP–Akt–YFP versus YFP–Akt with a P value < 0.0034, $n = 12$ cells at 95 % confidence interval. (**D**) Schematic model of Akt conformational change upon PDGF stimulation. FRET indicates a 'closed' conformation (without PDGF) and loss of FRET an 'open' conformation (with PDGF). The red dot on YFP represents the red-shifted version of EYFP (mutation $Gln^{70} \rightarrow$ Met).

PKB/Akt. To exploit EAF-induced FRET monitored by FLIM in intact cells, a double fluorescent-tagged GFP–Akt–YFP construct was designed and transiently transfected in NIH3T3 cells. We have shown that the GFP and YFP tags do not infringe upon the functional integrity of Akt protein. The translocation of the GFP–Akt–YFP construct at the plasma membrane was not altered compared with the single-tagged GFP–Akt and YFP–Akt constructs. Furthermore, the integrity of the activation of the double-tagged Akt protein was not compromised, as we could detect the expected inducible phosphorylation of the two regulatory sites, Thr^{308} and Ser^{473} phosphorylation and also the phosphorylation of a downstream substrate GSK3β. The transfer of energy between the GFP donor and red-shifted YFP acceptor within the GFP–Akt–YFP construct was measured under non-stimulated conditions. However, a loss of the FRET was monitored after PDGF stimulation at the plasma membrane. Therefore we conclude that the loss of the energy transfer was due to a change in the conformation of Akt from a 'closed' conformation (occurrence of FRET) in the basal condition to an 'open' conformation (loss of FRET) on PDGF treatment.

The activation of Akt after growth-factor stimulation has been shown to be strictly dependent on its translocation to the plasma membrane and on the phosphorylation of its regulatory

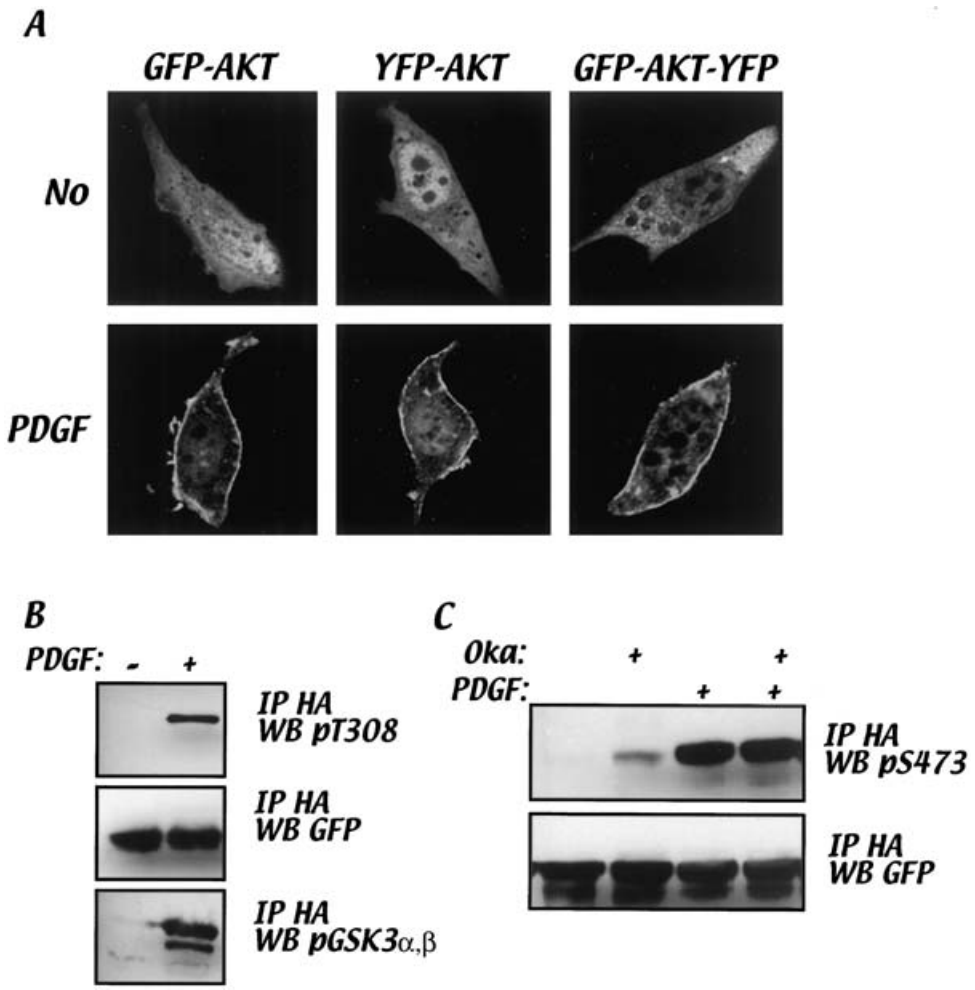

Figure 3 Functional integrity of the GFP–Akt–YFP construct

(**A**) Plasma-membrane localization of GFP–Akt, YFP–Akt and GFP–Akt–YFP constructs in NIH3T3 cells by confocal microscopy upon 5 min of PDGF stimulation (30 ng/ml). In each cell the mid-*z*-slice was taken. (**B**) The phosphorylation of immunoprecipitated Akt on Thr^{308} in GFP–Akt–YFP-transfected cells upon 5 min PDGF stimulation (30 ng/ml) (top panel) was assessed by Western blots with a phosphospecific antibody (WB phospho-Thr^{308}; see the Experimental section). Expression of the construct was verified by re-probing with an anti-GFP antibody (middle panel). The enzymic activity of the GFP–Akt–YFP construct was assessed by detecting recombinant GSK3 phosphorylation (bottom panel; see the Experimental section). (**C**) The phosphorylation of GFP–Akt–YFP on Ser^{473} upon PDGF (30 ng/ml for 5 min) or okadaic acid (Oka) treatment (1 μM for 90 min) was detected by Western blots (WB) using an anti-phospho-Ser^{473} antibody after immunoprecipitation (IP) with an anti-(haemagglutinin A) antibody (top panel). The expression of the GFP–Akt–YFP construct was verified by re-probing with an anti-GFP antibody (bottom panel).

sites Thr^{308} and Ser^{473} (on Akt1) by upstream kinase(s) [15,16]. The translocation of Akt was dependent on the integrity of its PH domain, which interacts with the lipid products of the phosphoinositide 3-kinase pathway. However, *in vitro*, an increase in the activity of Akt has been measured when the PH domain was deleted ('ΔPH-Akt') [17], implying that the PH domain negatively regulates the basal Akt kinase activity. A hypothesis to explain the dual role of the PH domain was that, *in vivo*, its association with the 3′-phosphoinositides after translocation at the plasma membrane upon activation induced an Akt conformational change that would release its inhibitory action. This conformational change could be stabilised by subsequent phosphorylation of Akt by upstream kinases, or could act to promote such phosphorylation. These latter issues will be the subject of future studies using the GFP-Akt-YFP construct. Recently, the crystal structure of the Akt kinase domain has been published and a mechanism for Akt activation involving a change in conformation of the hydrophobic C-terminal motif dependent on Thr^{308} and Ser^{473} phophorylations demonstrated [9]. However, in the crystallisation studies the suggested role of the PH domain in a conformational change of Akt, referred to above, could not be assessed, because the Akt PH domain had to be deleted for the purposes of crystallisation.

We demonstrate that this change in Akt conformation upon PDGF stimulation is dependent on the production of the 3′-phosphoinositide products of phosphoinositide 3-kinase, since it is largely prevented by treatment with an inhibitor of phosphoinositide 3-kinase, which also decreased the translocation of Akt to the plasma membrane. We have illustrated that *in situ* changes in protein conformation can be monitored in their physiological environment. We show that GFP–Akt–YFP retains properties associated with Akt itself and can be exploited to report on conformational changes through altered FRET. We therefore conclude that Akt indeed undergoes a

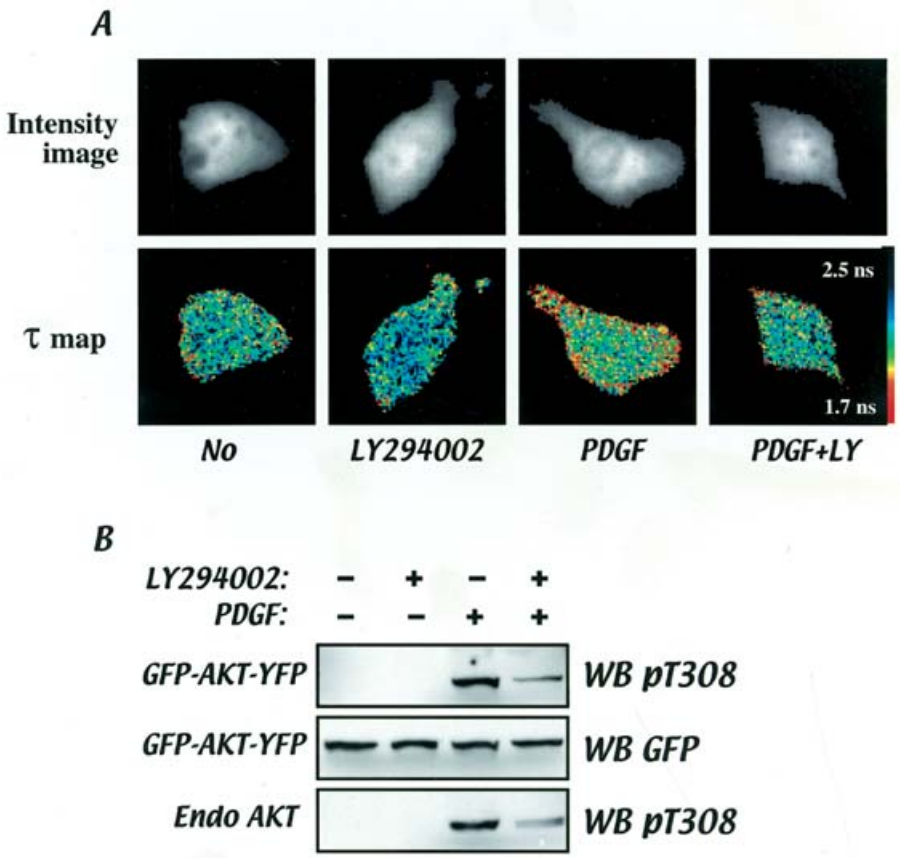

Figure 4 GFP–Akt–YFP conformational change is phosphoinositide 3-kinase-dependent

(**A**) Intensity images (top panel) and their corresponding average lifetime $\langle\tau\rangle$ maps (bottom panel) of GFP–Akt–YFP-transfected NIH3T3 cells. Cells were pretreated for 30 min with 50 μM LY294002 (phosphoinositide 3-kinase inhibitor) where indicated prior to 5 min PDGF stimulation at 30 ng/ml. The lifetime distribution ranges from 1.7 ± 0.15 ns to 2.5 ± 0.15 ns. Upon stimulation there is a loss of FRET ('open' conformation) at the plasma membrane indicated by the decrease in the GFP–Akt–YFP lifetime. In the presence of LY294002, this phenomenon is partially prevented. (**B**) Western-blot analysis of Akt Thr^{308} phosphorylation of GFP–Akt–YFP-transfected NIH3T3 cells treated with LY294002 and PDGF as indicated (top panel). The expression level of GFP–Akt–YFP is verified by Western blotting with an anti-GFP antibody (middle panel) and the Thr^{308} phosphorylation of endogenous Akt protein is shown as a control (bottom panel).

conformational change at the plasma membrane and suggest that this approach of monitoring *in situ* conformational changes can be utilized for other proteins, including related AGC kinase family members.

We thank Professor Peter J. Parker (Cancer Research UK) and Dr Anthony D. Postle (University of Southampton) for critically reading the manuscript before its submission, and Dr Rob Colley and Gareth Marsh (Cancer Research UK) for image treatment and information-technology support. This work was supported, in part, by Biotechnology and Biological Sciences Research Council (BBSRC) grant 28/B14728 and Cancer Research UK grant C133/A1812.

REFERENCES

1 Pearl, L. H. and Barford, D. (2002) Regulation of protein kinases in insulin, growth factor and Wnt signalling. Curr.Opin. Struct. Biol. **12**, 761–767
2 Harpur, A. G., Wouters, F. S. and Bastiaens, P. I. (2001) Imaging FRET between spectrally similar GFP molecules in single cells. Nat. Biotechnol. **19**, 167–169
3 Larijani, B., Allen-Baume, V., Morgan, C. P., Li, M. and Cockcroft, S. (2003) EGF regulation of PITP dynamics is blocked by inhibitors of phospholipase C and of the Ras-MAP kinase pathway. Curr. Biol. **13**, 78–84
4 Hughes, W. E., Larijani, B. and Parker, P. J. (2002) Detecting protein-phospholipid interactions. Epidermal growth factor-induced activation of phospholipase D1b *in situ*. J. Biol. Chem. **277**, 22974–22979
5 Thomas, C., Deak, M., Alessi, D. and van Aalten, D. (2002) High-resolution structure of the pleckstrin homology domain of protein kinase B/Akt bound to phosphatidylinositol (3,4,5)-trisphosphate. Curr. Biol. **12**, 1256–1262
6 Parker, P. J. and Parkinson, S. J. (2001) AGC protein kinase phosphorylation and protein kinase C. Biochem. Soc. Trans. **29**, 860–863
7 Alessi, D. R., Andjelkovic, M., Caudwell, B., Cron, P., Morrice, N., Cohen, P. and Hemmings, B. A. (1996) Mechanism of activation of protein kinase B by insulin and IGF-1. EMBO J. **15**, 6541–6551
8 Yang, J., Cron, P., Good, V. M., Thompson, V., Hemmings, B. A. and Barford, D. (2002) Crystal structure of an activated Akt/protein kinase B ternary complex with GSK3-peptide and AMP-PNP. Nat. Struct. Biol. **9**, 940–944
9 Yang, J., Cron, P., Thompson, V., Good, V. M., Hess, D., Hemmings, B. A. and Barford, D. (2002) Molecular mechanism for the regulation of protein kinase B/Akt by hydrophobic motif phosphorylation. Mol. Cell **9**, 1227–1240
10 Watton, S. J. and Downward, J. (1999) Akt/PKB localisation and 3′ phosphoinositide generation at sites of epithelial cell–matrix and cell–cell interaction. Curr. Biol. **9**, 433–436
11 Hofmann, T., Schaefer, M., Schultz, G. and Gudermann, T. (2002) Subunit composition of mammalian transient receptor potential channels in living cells. Proc. Natl. Acad. Sci. U.S.A. **99**, 7461–7466
12 Griesbeck, O., Baird, G. S., Campbell R. E., Zacharias D. A. and Tsien R. Y. (2001) Reducing the environmental sensitivity of yellow fluorescent protein. Mechanism and applications. J. Biol. Chem. **276**, 29188–29194
13 Lakowicz, J. R. (1999) Principles of Fluorescence Spectroscopy: Energy Transfer, 2nd edn., pp. 380–383, Kluwer Academic Plenium Publishers, New York

14 Ameer-Beg, S. M., Barber, P. R., Hodgkiss, R. J., Locke R. J., Newman R. G., Tozer G. M., Vojnovic, B. and Wilson, J. (2002) Application of multiphoton steady-state and lifetime imaging to mapping of tumour vascular architecture *in vivo*. Proc. SPIE Int. Soc. Opt. Eng. **4620**, 85–95
15 Aoki, M., Batista, O., Bellacosa, A., Tsichlis, P. and Vogt, P. K. (1998) The Akt kinase: molecular determinants of oncogenicity. Proc. Natl. Acad. Sci. U.S.A. **95**, 14950–14955
16 Alessi, D. R., James, S. R., Downes, C. P., Holmes, A. B., Gaffney, P. R., Reese C. B. and Cohen, P. (1997) Characterization of a 3-phosphoinositide-dependent protein kinase which phosphorylates and activates protein kinase Bα. Curr. Biol. **7**, 261–269
17 Sable, C. L., Filippa, N., Filloux, C., Hemmings, B. A. and Van Obberghen, E. (1998) Involvement of the pleckstrin homology domain in the insulin-stimulated activation of protein kinase B. J. Biol. Chem. **273**, 29600–29606

Received 5 March 2003/27 March 2003; accepted 27 March 2003
Published as BJ Immediate Publication 27 March 2003, DOI 10.1042/BJ20030358